THE JOURNAL OF BIOLOGICAL CHEMISTRY VOL. 288, NO. 26, pp. 18894–18902, June 28, 2013

Reinterpreting the Action of ATP Analogs on K_{ATP} Channels*

Received for publication, April 11, 2013, and in revised form, May 1, 2013 Published, JBC Papers in Press, May 12, 2013, DOI 10.1074/jbc.M113.476887

David Ortiz[‡], Lindsay Gossack[‡], Ulrich Quast[§], and Joseph Bryan[‡1]

From the [‡]Pacific Northwest Diabetes Research Institute, Seattle, Washington 98122 and the [§]Department of Pharmacology and Experimental Therapy, Institute of Experimental and Clinical Pharmacology and Toxicology, Eberhard-Karls-University Hospitals and Clinics, Wilhelmstrasse 56, D-72074 Tübingen, Germany

Background: Stimulation by post-hydrolytic, ADP-bound conformations of SUR1 underlies current models of K_{ATP} channel activation; ATP analogs are assumed to lower activity by reducing hydrolysis.
Results: ATPγS switches conformations with lowered affinity; AMP-PxP selectively bind NBD1, preventing switching.
Conclusion: The actions of ATP analogs on K_{ATP} channels require reinterpretation.
Significance: Reduced affinities of SUR1 NBDs for ATP analogs limit conformational switching and channel activity.

Neuroendocrine-type K_{ATP} channels, $(SUR1/Kir6.2)_4$, couple the transmembrane flux of K^+, and thus membrane potential, with cellular metabolism in various cell types including insulin-secreting β-cells. Mutant channels with reduced activity are a cause of congenital hyperinsulinism, whereas hyperactive channels are a cause of neonatal diabetes. A current regulatory model proposes that ATP hydrolysis is required to switch SUR1 into post-hydrolytic conformations able to antagonize the inhibitory action of nucleotide binding at the Kir6.2 pore, thus coupling enzymatic and channel activities. Alterations in SUR1 ATPase activity are proposed to contribute to neonatal diabetes and type 2 diabetes risk. The regulatory model is partly based on the reduced ability of ATP analogs such as adenosine 5′-(β,γ-imino)triphosphate (AMP-PNP) and adenosine 5′-*O*-(thiotriphosphate) (ATPγS) to stimulate channel activity, presumably by reducing hydrolysis. This study uses a substitution at the catalytic glutamate, $SUR1_{E1507Q}$, with a significantly increased affinity for ATP, to probe the action of these ATP analogs on conformational switching. ATPγS, a slowly hydrolyzable analog, switches SUR1 conformations, albeit with reduced affinity. Nonhydrolyzable AMP-PNP and adenosine 5′-(β,γ-methylenetriphosphate) (AMP-PCP) alone fail to switch SUR1, but do reverse ATP-induced switching. AMP-PCP displaces 8-azido-[^{32}P]ATP from the noncanonical NBD1 of SUR1. This is consistent with structural data on an asymmetric bacterial ABC protein that shows that AMP-PNP binds selectively to the noncanonical NBD to prevent conformational switching. The results imply that MgAMP-PNP and MgAMP-PCP (AMP-PxP) fail to activate K_{ATP} channels because they do not support NBD dimerization and conformational switching, rather than by limiting enzymatic activity.

Neuroendocrine ATP-sensitive K^+ channels, $(SUR1/Kir6.2)_4$, couple membrane electrical activity with cell metabolism in neurons and many endocrine cells, including pancreatic islet α-, β-, and δ-cells (see Ref. 1 for review). These channels respond to changes in the levels of MgATP and ADP, which have both inhibitory and stimulatory actions. Nucleotides bind to Kir6.2[2] to reduce the channel open probability, whereas ATP interactions with SUR1 antagonize this inhibitory effect. These nucleotide effects are modulated by other factors including phosphoinositides (2–9) and long-chain acyl-CoAs (10–16). SUR1, the channel regulatory subunit, is an enzyme, a member of the ATP-binding cassette (ABC) family of proteins that utilize the energy of ATP binding and hydrolysis to transport substrates across cell membranes (17, 18). A current model of K_{ATP} channel regulation assumes that a post-hydrolytic, ADP-bound enzymatic intermediate or conformation of SUR1 stimulates channel openings, *i.e.* that hydrolysis is essential for activation (Ref. 19 and reviewed in (20–22). This model is based in part on studies demonstrating that nonhydrolyzable ATP analogs such as AMP-PNP and AMP-PCP fail to stimulate channel activity, whereas the slowly hydrolyzable ATPγS stimulates less efficiently than ATP (23–30).

Contrary to the current model, we observed that the *binding* of ATP, without hydrolysis, is sufficient to switch SUR1 from conformations with high affinity for glibenclamide (GBC), a K_{ATP} channel antagonist, to conformations with reduced antagonist affinity, but a markedly enhanced affinity for the channel agonist diazoxide, *i.e.* from nonstimulatory to stimulatory states (31). ATP^{4-}, in the absence of Mg^{2+} required for enzymatic activity (17), efficiently switched the conformations of wild-type (WT) SUR1 and mutant receptors known to hyperactivate Kir6.2 pores and thus cause neonatal diabetes (ND).

The ND mutant receptors, $SUR1_{Q1178R}$ and $SUR1_{R1182Q}$, substitutions outside the nucleotide-binding domains (NBDs), have increased affinities for MgATP and ATP^{4-}, consistent with their spending more time in stimulatory conformations able to increase channel activity. Structural studies on multiple

* This work was supported by American Diabetes Association Grant ADA 1-10-BS21 (to J. B.).

[1] To whom correspondence should be addressed: Pacific Northwest Diabetes Research Institute, 720 Broadway, Seattle, WA, 98122. Tel.: 206-568-1462; E-mail: jbryan@pnri.org.

[2] The abbreviations used are: Kir6.2, potassium inward rectifier type 6.2; SUR1, sulfonylurea receptor type 1; ABC, ATP-binding cassette; GBC, glibenclamide; ND, neonatal diabetes; NBD, nucleotide-binding domain; ATPγS, adenosine 5′-*O*-(thiotriphosphate); AMP-PNP, adenosine 5′-(β,γ-imino)triphosphate; AMP-PCP, adenosine 5′-(β,γ-methylenetriphosphate); MgAMP-PNP, Mg-5′-adenylyl imidodiphosphate; MgAMP-PCP, Mg-adenylyl (β,γ-methylene) diphosphonic acid; AMP-PxP, MgAMP-PNP and MgAMP-PCP.

ABC proteins show that ATP binding to the NBDs induces the formation of an NBD dimer with two ATP molecules sandwiched in the dimer interface. Dimerization drives reconfiguration of the transmembrane helix bundles from inward-to-outward-facing conformations (reviewed in Refs. 32 and 33). Therefore we proposed that ATP binding and NBD dimerization, without hydrolysis, drive SUR1 from a nonstimulatory, inward-facing conformation with highest affinity for GBC to an outward-facing stimulatory state with >10-fold reduced affinity for GBC and >100-fold increased affinity for channel agonists (31).

AMP-PNP stabilizes NBD dimers of *symmetric* ABC proteins in outward-facing configurations with two bound nucleotides (34, 35). On the other hand, the structure of an asymmetric ABC protein, TM287/288 from *Thermotoga maritima*, shows a single AMP-PNP bound to an inward-facing conformation (36). Therefore the action of AMP-PNP and AMP-PCP on ATP-induced switching of SUR1, which like several other ABC proteins has asymmetric NBDs (Refs. 37–39 and see Ref. 40 for review), was analyzed. The sensitivity of the analysis was improved by using SUR1 substitutions with increased affinities for ATP. These include $SUR1_{Q1178R}$ identified with hyperactive K_{ATP} channels in an ND patient (41, 42) and $SUR1_{E1507Q}$. The Glu → Gln substitution, in the highly conserved catalytic glutamate of SUR1 NBD2, dramatically reduces enzymatic activity (≥500-fold) in other ABC proteins (43, 44) and is used in structural studies to stabilize or trap ABC proteins in outward-facing, nucleotide-bound conformations with dimerized NBDs (45–47). Under equilibrium conditions, we found that $SUR1_{E1507Q}$ binds ATP^{4-} nearly 150 times more tightly than WT, showing that charge at position 1507 in the conserved Walker B phosphate-binding domain is a significant determinant of nucleotide affinity. For comparison, the affinity of $SUR1_{Q1178R}$, a substitution outside the NBDs, is intermediate between WT and E1507Q. The inclusion of Mg^{2+} increases the affinity for ATP by ≥100-fold.

ATPγS fully supports switching with or without Mg^{2+}, but SUR1 has a reduced affinity for this analog *versus* ATP. In contrast, MgAMP-PNP and MgAMP-PCP (AMP-PxP) alone do not affect GBC binding at high concentration, but fully reverse the action of added MgATP in a dose-dependent manner. Additionally, AMP-PCP displaces 8-azido-[^{32}P]ATP from the noncanonical NBD1 of SUR1. The results are consistent with studies on two other asymmetric ABC proteins that demonstrate that AMP-PNP selectively binds the noncanonical NBD1 of cystic fibrosis transmembrane conductance regulator (CFTR) with high affinity, but binds NBD2 with much lower affinity (48, 49), and interacts selectively with the noncanonical NBD of TM287/288 to stabilize an inward-facing conformation (36). We propose that AMP-PxP act on SURs to reduce channel activity by stabilizing an inward-facing conformation, and thus the actions of AMP-PxP reflect the asymmetry of SURs, rather than inhibition of ATP hydrolysis *per se*.

EXPERIMENTAL PROCEDURES

The procedures used to express WT and mutant SUR1 in *Pichia pastoris*, to isolate membranes, and to carry out ^{3}H-labeled GBC binding experiments were described previously (31). An additional wash step was added in the membrane isolation protocol to reduce carryover of endogenous nucleotides.

[^{3}H]GBC Binding Inhibition Experiments—^{3}H-labeled GBC was held fixed at 1 nM, and the reactions included the indicated concentrations of nucleotides. Experiments with MgATP (free $[Mg^{2+}] > 1$ mM) included a creatine phosphokinase-based ATP-regenerating system to maintain a constant concentration of ATP over the 30-min incubation (50). The stability of ATP levels was verified using luciferase assays (Sigma). Experiments with MgADP included 10 mM AMP to inhibit endogenous adenylate kinases to reduce ATP production. Experiments with MgADP and MgATP analogs, where a regenerating system was not required, included 1 mM free Mg^{2+}. Mg^{2+}-free experiments included 1 mM EDTA. Nonspecific binding was determined in the presence of 1 μM unlabeled GBC and was typically 15% of total binding. The results are plotted as

$$\text{Specific bound GBC} = \frac{\text{specific bound } (+X)}{\text{specific bound } (-X)} \qquad \text{(Eq. 1)}$$

where X is the reagent whose effect is being assayed, *e.g.* ± ATP^{4-}, etc.

Photolabeling— 8-azido-[^{32}P]ATP photolabeling and densitometry were done as described previously (31).

Allosteric Analysis—The equations for the equilibrium models were derived following Wyman and Gill (51); the algebraic manipulations were done using *Mathematica* (Wolfram Research, Champaign, IL). The binding equations were derived from the binding partition functions, the sum of the contributions of the different species relative to one reference species, taken here as the unliganded receptor, R. The eight-state allosteric model shown in Fig. 4*C* is used as an example. The model describes the linkage between the equilibrium binding of MgAMP-PNP (A), ^{3}H-labeled GBC (G), and MgATP (T) on $SUR1_{E1507Q}$ (R). K_A is the equilibrium dissociation constant for binding of A, K_G is the constant for G, and K_1 and K_2 are the constants for the binding of T to NBD1 and NBD2, respectively. α, β, and γ are allosteric constants. $\alpha = \gamma = 1$ because previous data indicate that binding of nucleotide to NBD1 alone does not alter GBC binding (31). β is the allosteric constant reflecting the linkage between GBC binding and structural changes associated with occupation of both NBDs. For $\beta > 1$, nucleotide binding reduces the affinity of SUR1 for sulfonylureas. The partition function for the eight-state model is

$$P = \frac{[R] + [RA] + [RG] + [{}_TR] + [{}_TR_T] + [{}_TRG] + [{}_TR_TG] + [{}_ARG]}{[R]} \qquad \text{(Eq. 2)}$$

where ${}_TR$ and ${}_TR_T$ indicate binding at NBD1 and both NBD1 and NBD2, respectively. Substituting dissociation constants gives the binding polynomial.

$$P = 1 + \frac{A}{K_A} + \frac{G}{K_G} + \frac{T}{K_1} + \frac{T^2}{K_1K_2} + \frac{GT}{\alpha K_1K_G} + \frac{GT^2}{\beta K_1K_2K_G} + \frac{AG}{\gamma K_AK_G} \qquad \text{(Eq. 3)}$$

$\bar{G}$, the amount of ^{3}H-labeled GBC specifically bound per mole of SUR1, which is dependent on [G], [T], and [A], is given by

$$\bar{G} = \frac{\partial \ln P}{\partial \ln G} = \frac{[G]}{P}\frac{\partial P}{\partial G} \qquad \text{(Eq. 4)}$$

where

$$\bar{G} = \frac{G\left(\frac{1}{K_G} + \frac{T}{\alpha K_1 K_G} + \frac{T^2}{\beta K_1 K_2 K_G} + \frac{A}{\gamma K_A K_G}\right)}{1 + \frac{A}{K_A} + \frac{G}{K_G} + \frac{T}{K_1} + \frac{T^2}{K_1 K_2} + \frac{GT}{\alpha K_1 K_G} + \frac{GT^2}{\beta K_1 K_2 K_G} + \frac{AG}{\gamma K_A K_G}} \qquad \text{(Eq. 5)}$$

The plotted experimental variable, specific bound GBC, is defined as $\bar{G}/\bar{G}_{no\ ATP}$. Parameters were estimated using nonlinear fit models in the *Mathematica* environment with $\alpha = \gamma = 1$ and predetermined values of β, K_G, and G.

The equation for the four-state equilibrium model is.

$$\bar{G} = \frac{G\left(\frac{1}{K_G} + \frac{T}{\beta K_G K_T}\right)}{1 + \frac{G}{K_G} + \frac{T}{K_T} + \frac{GT}{\beta K_G K_T}} \qquad \text{(Eq. 6)}$$

Fittings were estimated using predetermined values for K_G.

Statistics—Where indicated, the IC_{50} values were estimated by fitting a logistic equation. The means ± S.E. are plotted; the number of replicate experiments varies, but $n \geq 3$ in all cases.

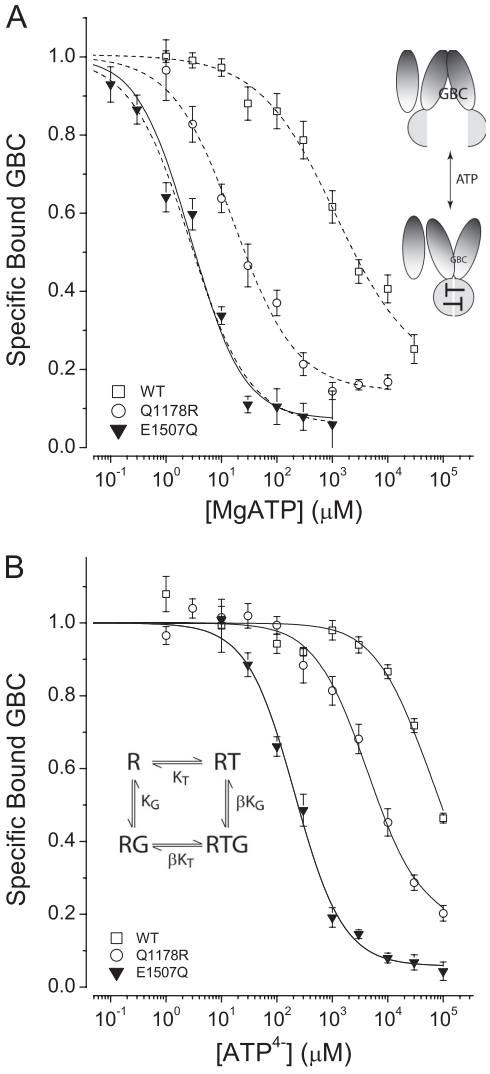

FIGURE 1. **ATP-induced conformational switching of SURs.** *A*, the effect of MgATP on GBC binding. *Dashed curves* are fits to a logistic equation used to estimate the IC_{50} values (in μM): WT: 1163 ± 439, slope = 0.8 ± 0.1; Q1178R: 17 ± 3, slope = 0.8 ± 0.1; E1507Q: 2.7 ± 0.4, slope = 0.8 ± 0.1. IC_{50} mean ± S.E., slope mean ± S.E., n = 3–20. The *solid curve* for $SUR1_{E1507Q}$ is the best fit to the four-state model shown in the *inset*. The parameters are $K_T = 1$ μM and $\beta = 40$ with a defined value for $K_G = 0.63$ nM. *B*, the effect of ATP^{4-} on GBC binding. The curves are the best fits to the four-state model. The parameters are K_T = 94, 2550, and 13,400 μM and β = 40, 9.2, and 15.1 with K_G defined as 0.63, 1.0, and 0.25 nM, for E1507Q, Q1178R, and WT, respectively. Here and in the following figures, the graphics suggest the conformational changes in SUR1 upon binding of nucleotides.

RESULTS

ATP-induced Conformational Switching of WT and Mutant SUR1—The effect of ATP on SUR1 conformation was determined using GBC as a conformational probe. Fig. 1 shows that ATP, with or without Mg^{2+}, has a strong negative effect on GBC binding. ATP effectively switches WT and substituted SURs from inward-facing conformations with highest affinities for GBC to outward-facing states with reduced affinities as shown schematically. The apparent differences in affinity, judged for example by their IC_{50} values (*panel A* and Table 1), is ~430-fold for WT *versus* $SUR1_{E1507Q}$; the value for $SUR1_{Q1178R}$, characterized previously, is intermediate (31). Comparison of *panels A* and *B* shows that Mg^{2+} significantly increases the apparent affinity of all three receptors for ATP.

The E1507Q and Q1178R substitutions do not have large effects on the affinities of the apo-receptors for GBC, given by the dissociation constants (K_G), which are determined in independent experiments (Table 1). To characterize the negative allosteric linkage between binding sites in $SUR1_{E1507Q}$, we assume that hydrolysis is negligible both in the presence and in the absence of Mg^{2+} (43, 44). A four-state equilibrium model (Fig. 1, *inset*) was used to estimate the affinities for ATP (K_T) and the allosteric constants (β). The results are tabulated in Table 1 along with the IC_{50} values. The four-state model has not been used to analyze the MgATP effects on WT and $SUR1_{Q1178R}$, which are potentially in an enzymatic steady state. In Fig. 1, the *solid lines* are the best-fit curves derived from the

TABLE 1

Binding parameters (K_G, IC_{50}, and K_T values) for WT, Q1178R, and E1507Q

K_G values are nM; all IC_{50} and K_T values are μM. —, not detectable.

		IC_{50}		K_T			
	K_G	MgATP	MgADP	MgATP (β)	ATP^{4-} (β)	MgATPγS (β)	$ATP\gamma S^{4-}$ (β)
WT	0.25 ± 0.02	1163 ± 439	161 ± 28	—	13,400 ± 3360 (15.1 ± 9.4)	—	—
Q1178R	1.0 ± 0.1	17 ± 3	25 ± 2	—	2550 ± 290 (9.2 ± 1.4)	—	—
E1507Q	0.63 ± 0.16	2.7 ± 0.4	—	1 ± 0.2 (40 ± 3)	94 ± 8 (40 ± 1)	29 ± 7 (11.6 ± 3)	234 ± 31 (3.2 ± 0.1)

four-state model. The fits were constrained using the values for K_G, the dissociation constants for GBC binding to the apo-receptors (Table 1). The product of the allosteric constant, β, and K_G determines the plateau values at saturating concentrations of nucleotide and is the dissociation constant for GBC binding to the fully ATP-liganded receptor. The estimates of β for WT and $SUR1_{Q1178R}$ are consistent with fully ATP-liganded, outward-facing receptors having approximately a 10-fold lower affinity for GBC (31). The value for $SUR1_{E1507Q}$, 40, is significantly greater, implying that the affinity of fully ATP-liganded $SUR1_{E1507Q}$ for GBC is considerably reduced, *i.e.* 0.63 *versus* 25 nM, unliganded *versus* liganded, respectively.

ATP^{4-} switches the conformation of WT and mutant receptors. Fig. 1*B* shows a significant difference, ~27-fold, in the affinities of $SUR1_{E1507Q}$ *versus* $SUR1_{Q1178R}$ for ATP^{4-}. The effect of nucleotide on WT is not saturated, but the estimated affinity of $SUR1_{E1507Q}$ is ~150-fold greater than WT (Table 1). The structural difference between $SUR1_{E1507Q}$ and WT (Glu-1507) is the elimination of the negative charge at position 1507. The results imply that electrostatic interactions between phosphate residues and the carboxyl group at position 1507 is a significant determinant of nucleotide affinity. Neutralizing the charge significantly increases the binding energy by ~3 kcal/mol at 37 °C, $SUR1_{E1507Q}$ *versus* WT. The general finding that added Mg^{2+}, bound to the β and γ phosphates, increases the apparent affinity supports this idea.

Comparing the affinities of $SUR1_{E1507Q}$ for MgATP *versus* ATP^{4-} shows that the receptor binds MgATP ~100-fold more tightly than ATP^{4-}. Thus the addition of Mg^{2+} contributes ~2.8 kcal/mol to the binding energy at 37 °C. The WT and $SUR1_{Q1178R}$ receptors show a semiquantitatively similar Mg^{2+} effect when comparing the IC_{50} values for MgATP *versus* K_T for ATP^{4-} (Table 1). It is worth noting that nucleotide binding and GBC binding are negatively linked allosteric functions; thus the GBC (1 nM) used to assess conformational changes reduces the *apparent* affinity for nucleotide, *i.e.* "right shifts" the response curves. This is apparent, for example, for $SUR1_{E1507Q}$ where the IC_{50} is ~3-fold greater than the estimated K_T value.

MgADP-induced Switching—Fig. 2 shows that $SUR1_{E1507Q}$ has a reduced affinity for MgADP when compared with WT SUR1. The membrane preparations have significant endogenous adenylate kinase activity able to convert MgADP to ATP. This activity is suppressed by the addition of AMP (10 mM). ATP measurements using luciferase show that the concentration of ATP is ~4 μM when the concentration of MgADP is 300 μM (31). Thus at the highest concentration, 1 mM MgADP, a fraction of the switching is due to ATP.

It is worth noting that although the E1507Q substitution has not been associated with disease, the E1507D substitution, also expected to have impaired ATPase activity, is a cause of ND. The $SUR1_{E1507D}$/Kir6.2 channels exhibit a comparable reduced sensitivity to stimulation by MgADP (52). Interestingly, although the $SUR1_{E1507Q}$ substitution has a reduced affinity for MgADP, $SUR1_{Q1178R}$, which also hyperactivates Kir6.2 pores to produce ND, has a significantly higher apparent affinity for MgADP (31) (Fig. 2).

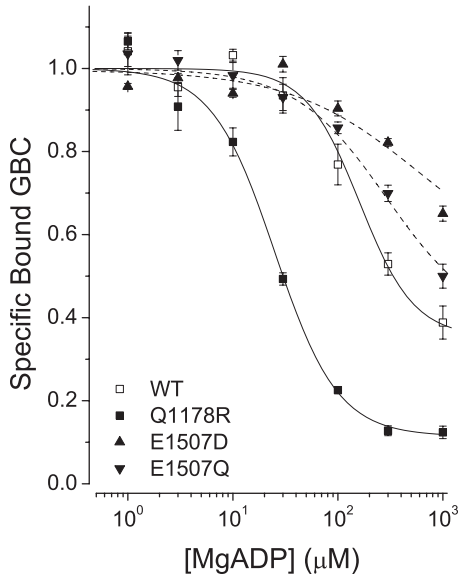

FIGURE 2. **MgADP-induced conformational switching of SURs.** The *solid lines* are fits to a logistic equation: IC_{50} values: WT: 161 ± 28, slope = 1.7 ± 0.4; Q1178R: 25 ± 2, slope = 1.5 ± 0.1. Values are means ± S.E., $n > 10$. *Dashed lines* are drawn through the data points for $SUR1_{E1507D}$ and $SUR1_{E1507Q}$. The apparent affinity for this receptor is difficult to estimate. Its affinity for MgADP is lower than WT, whereas its affinity for MgATP is significantly higher, and thus a significant fraction of the switching above 300 μM ADP may reflect the conversion of ADP to ATP by endogenous adenylate kinase in the membrane preparations.

ATPγS, a Slowly Hydrolyzable ATP Analog, Switches SUR1 Conformations with Reduced Affinity—ATPγS, an analog of ATP with one oxygen of the γ-phosphate replaced by a sulfur atom, is slowly utilized by a variety of kinases and ATPases (53). In the current regulatory model, reduced enzymatic activity would slow transition to a post-hydrolytic stimulatory conformation. This idea was tested by assessing the action of ATPγS on GBC binding under steady state and equilibrium conditions (± Mg^{2+}). Fig. 3*A* compares the action of MgATP *versus* MgATPγS on conformational switching. $SUR1_{E1507Q}$ has a higher affinity for MgATP *versus* MgATPγS, estimated using a four-state equilibrium model. The dissociation constants (K_T) for ATP are 1.0 ± 0.2 *versus* 29 ± 7 μM, MgATP *versus* MgATPγS, respectively. To support the use of the four-state model and to assess the binding of $ATP\gamma S^{4-}$ directly, *i.e.* without Mg^{2+} present, the affinities of $SUR1_{E1507Q}$ for ATP^{4-} and $ATP\gamma S^{4-}$ were compared (Fig. 3*B*). The estimated K_T values were 94 ± 8 *versus* 234 ± 31 μM, for ATP^{4-} *versus* $ATP\gamma S^{4-}$, respectively. It is worth noting that the allosteric constants, β values, for the two nucleotides are significantly different. The final plateau at saturating concentrations of nucleotide determines this parameter. The β values used to specify the curves in Fig. 3*B* were 3.2 ± 0.1 *versus* 40 ± 1, for $ATP\gamma S^{4-}$ *versus* ATP^{4-}, respectively. The results show that ATPγS supports conformational switching of SUR1 and that the affinity for this analog is less than for ATP, with or without Mg^{2+}.

AMP-PNP and AMP-PCP Reverse the ATP-induced Conformational Switching of SUR1—Nonhydrolyzable ATP analogs, specifically MgAMP-PNP and MgAMP-PCP, are unable to activate K_{ATP} channels (19, 25, 54–56) and will reduce channel activity when MgATP is present (Ref. 19, but see Ref. 57). MgAMP-PNP and MgAMP-PCP are assumed not to hydrolyze

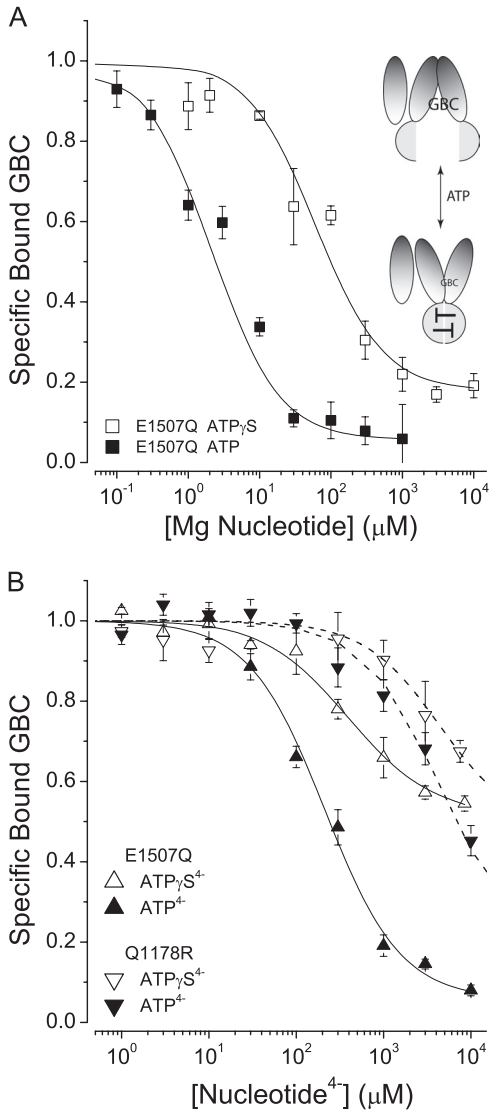

FIGURE 3. **SURs have reduced affinity for ATPγS versus ATP.** *A*, comparison of MgATPγS *versus* MgATP effects. The curves are best fits to a four-state model (Fig. 1*B*, *inset*). The best-fit dissociation constants are $K_T = 1$ and 29 μM for MgATP and MgATPγS, respectively. The β values are 40 and 11.6 for MgATP and MgATPγS, respectively. The dissociation constant, $K_G = 0.63$ nM for GBC, was determined independently. *B*, comparison of the affinities of $SUR1_{E1507Q}$ for ATP^{4-} *versus* $ATP\gamma S^{4-}$. The *solid curves* are the best fits to the four-state model; the parameters are $K_T = 94$ *versus* 234 μM; $\beta = 40$ *versus* 3.2, ATP^{4-} *versus* $ATP\gamma S^{4-}$, respectively. The dissociation constant for GBC, $K_G = 0.63$ nM, was fixed during fitting.

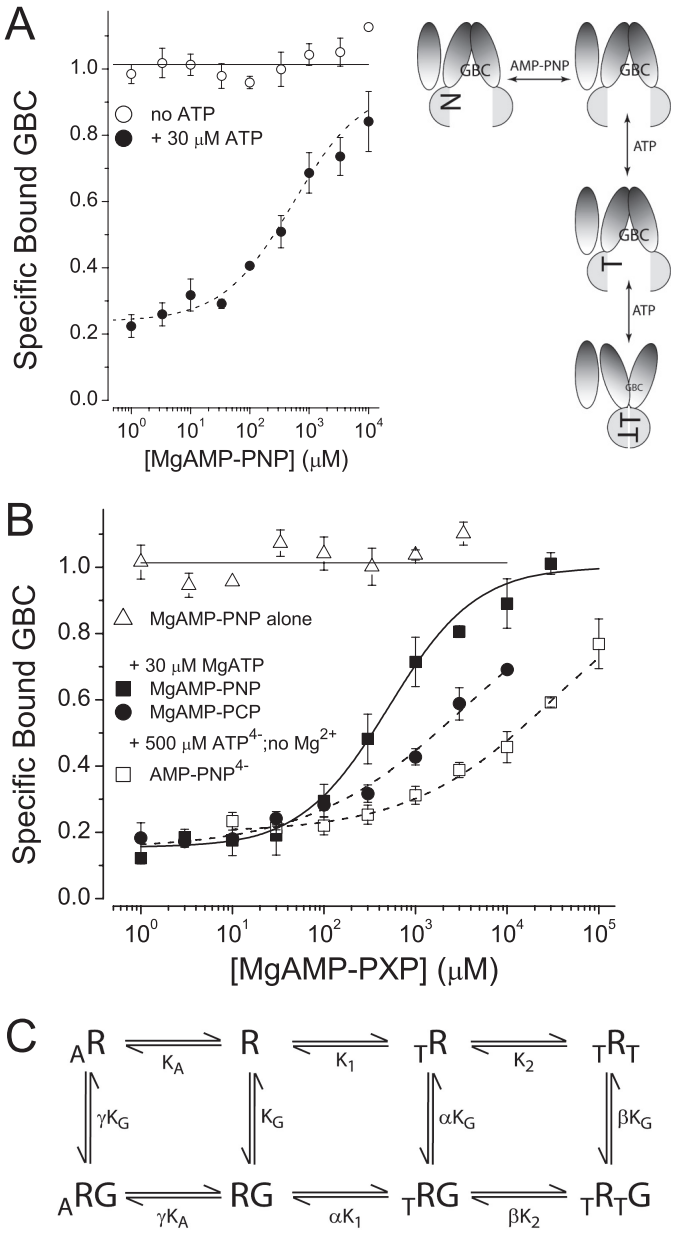

FIGURE 4. **AMP-PxP reverse ATP-induced conformational switching.** *A* and *B*, MgAMP-PNP alone does not affect the conformational state of $SUR1_{Q1178R}$ (*A*) or $SUR1_{E1507Q}$ (*B*). MgAMP-PNP reverses the conformational shift induced by MgATP (30 μM) in both SURs. MgAMP-PCP and AMP-PNP^{4-} also reverse, but the apparent affinities are lower. The *dashed lines* are logistic curves through the data points; the parameters are $S_{0.5} = 530 \pm 124$ μM for $SUR1_{Q1178R}$ (*A*). The $SUR1_{E1507Q}$ $S_{0.5}$ values in *B* are 573 ± 103, 3360 ± 410, and 31,100 ± 2240 μM for MgAMP-PNP, MgAMP-PCP, and AMP-PNP^{4-}, respectively. *C*, the *solid curve* in *B* for $SUR1_{E1507Q}$ is a fit to an eight-state model with the following parameters: $\alpha = \gamma = 1$, $\beta = 40$, $K_G = 0.63$ nM, $K_1 = 0.7 \pm 0.2$ μM, $K_2 = 1.5 \pm 0.1$ μM, $K_A = 1.2 \pm 0.2$ μM.

and thus prevent the transition of SUR to post-hydrolytic, stimulatory conformations (for review, see Refs. 20 and 21). MgAMP-PNP does dimerize the NBDs of symmetric ABC proteins (34, 35); thus we anticipated that it could switch SUR1. However, Fig. 4 shows that MgAMP-PNP at concentrations >100 times the IC_{50} values for MgATP (Fig. 1*A*) has no significant effect on GBC binding, *i.e.* AMP-PNP alone does not support conformational switching of either $SUR1_{Q1178R}$ (Fig. 4*A*) or $SUR1_{E1507Q}$ (Fig. 4*B*). AMP-PCP alone also has no effect. This could imply that AMP-PNP does not interact with SUR1 as suggested by others (57). To test this possibility, receptors were incubated with 30 μM MgATP (to "preswitch" them) and increasing concentrations of AMP-PNP or AMP-PCP. AMP-PNP concentration-dependently reverses the effect of MgATP on GBC binding, similar to an early observation by Schwanstecher *et al.* (58). Fig. 4 (*A* and *B*) shows the results for $SUR1_{Q1178R}$ and $SUR1_{E1507Q}$, respectively. As an additional control, these experiments were performed with and without the ATP-regenerating system present with similar results. Fig. 4*B* suggests that the affinity of $SUR1_{E1507Q}$ for AMP-PCP is ~10-fold less than for AMP-PNP. The reversal effect of AMP-PNP is not dependent on Mg^{2+}. AMP-PNP^{4-} effectively reverses the action of 500 μM ATP^{4-} (Fig. 4*B*).

TABLE 2

Binding parameters ($S_{0.5}$ and K_1, K_2, and K_A values) for Q1178R and E1507Q

Values are μM; K_1 and K_2, the affinities for MgATP at NBD1 and NBD2, respectively and K_A, the affinity for MgAMP-PNP at NBD1, were estimated using an eight-state model. —, not detectable.

	$S_{0.5}$					
SUR1	MgAMP-PNP	MgAMP-PCP	AMP-PNP^{4-}	K_1	K_2	K_A
Q1178R	530 ± 124	—	—	—	—	—
E1507Q	573 ± 103	3360 ± 410	31100 ± 2240	0.7 ± 0.2	1.5 ± 0.1	1.2 ± 0.2

An eight-state equilibrium model was used to estimate the linkage between the binding of AMP-PNP, ATP, and GBC on $SUR1_{E1507Q}$ (Fig. 4*C*, graphic). The model includes the binding of two ATP (T) molecules at the NBDs of SUR1 and the binding of a single GBC molecule (G). Based on the reversal experiments, and the observation of Hohl *et al.* (36) that AMP-PNP interacts with a single NBD in an asymmetric ABC protein to stabilize the inward-facing conformation, we assume that AMP-PNP (A) binds to NBD1 to stabilize inward-facing conformations of SUR1 with the highest affinity for GBC. The estimated binding parameters are reasonably consistent with the results in Fig. 1. The dissociation constant (K_2) for MgATP at NBD2 is ~1.5 μM, in agreement with ~1 μM determined in Fig. 1*B*. The dissociation constant (K_1) for MgATP at NBD1 is estimated at 0.7 μM, broadly consistent with estimates of IC_{50}, 10–40 μM, for 8-azido-[^{32}P]ATP^{4-} binding at NBD1 (31) and the observation that adding Mg^{2+} increases the affinity of nucleotide binding at NBD2 by ~100-fold. The fitting suggests that the dissociation constant (K_A) for MgAMP-PNP at NBD1 is similar to that for MgATP. The allosteric constant, $\beta = 40$, agrees with the estimates in Fig. 1. In Fig. 4 (*A* and *B*), the *dashed lines* are curves drawn through the points; no attempt has been made to fit an eight-state model to the partial saturation data for AMP-PCP and AMP-PNP^{4-} or for $SUR1_{Q1178R}$, which is potentially in steady state. The binding parameters are summarized in Tables 1 and 2.

AMP-PCP Interacts with NBD1—The model in Fig. 4 assumes that AMP-PxP bind to the asymmetric NBD1 of SUR1. To support this assumption, nucleotide competition experiments were carried out in the absence of Mg^{2+}, conditions where NBD1 of SUR1 has a significantly greater affinity for ATP (Refs. 59 and 60, and see also Ref. 31). An IC_{50} of 232 ± 25 μM was determined for the heterologous displacement of 8-azido-[α-^{32}P]ATP^{4-} by AMP-PCP^{4-} (Fig. 5). A K_i value (= 95 μM) was estimated using the Cheng-Prusoff relation (61) and K_D for azido-ATP^{4-} of ~0.7 μM estimated by homologous displacement of 8-azido-[α-^{32}P]ATP^{4-} by unlabeled 8-azido-ATP^{4-} (data not shown) The results are consistent with the idea that AMP-PxP bind to the asymmetric NBD1 of SUR1 and stabilize the inward-facing conformation.

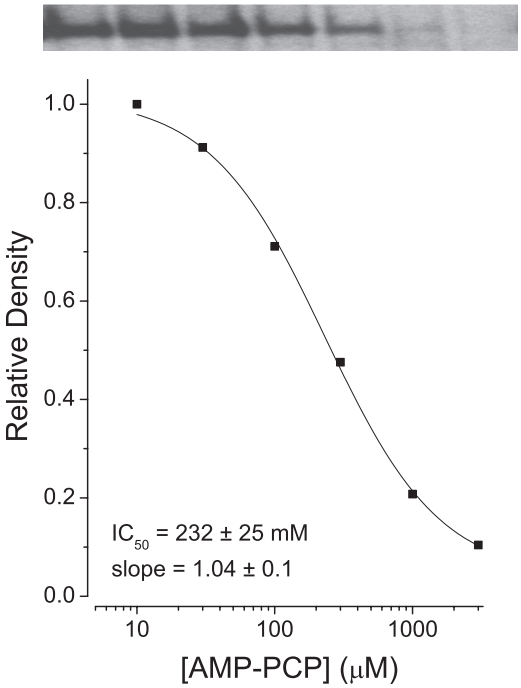

FIGURE 5. **Interaction of AMP-PCP with NBD1 of SUR1.** Membranes were incubated with 1 μM 8-azido-[α-^{32}P]ATP and increasing concentrations of unlabeled AMP-PCP and then analyzed as described previously (31). EDTA (2 mM) was added to chelate Mg^{2+}. Images of the scanned autoradiographs are shown. IC_{50} value was estimated by fitting a logistic equation. The IC_{50} value is 232 ± 25 μM, slope = 1.04 ± 0.1.

DISCUSSION

ATP has inhibitory and stimulatory actions on K_{ATP} channels. Nucleotide binding to the Kir pore reduces the probability of channel openings, whereas interactions with SUR1 antagonize this inhibition to stimulate channel activity. SUR1 is an ABC protein, and like other ABC proteins, is reported to have Mg^{2+}-dependent ATPase activity (17, 18). An ADP-bound, post-hydrolytic conformation of SUR1 is proposed to be the enzymatic intermediate that stimulates openings of ATP-inhibited Kir6.2 pores. By contrast, we observe that ATP binding, in the absence of Mg^{2+} needed for hydrolysis, is sufficient to switch the conformations of WT SUR1 and SUR1 ND mutants. The ATP-bound states are presumed to be stimulatory conformations based on pharmacologic criteria, *i.e.* their reduced affinity for GBC, a channel antagonist, and increased affinity for diazoxide, a channel agonist (31). The structures of multiple apo- and ATP-bound ABC proteins (reviewed in Refs. 33 and 35) imply that ATP binding switches SUR1 from inward-facing, nonstimulatory apo states to ATP-liganded, outward-facing stimulatory configurations. This is shown as a graphic in Fig. 1. The increased affinity of the ND mutant receptors for ATP implies that they will spend more time in stimulatory conformations and thus produce the hyperactive K_{ATP} channels characteristic of neonatal diabetes.

The inhibitory actions of ATP analogs have been used to support the current regulatory model by assuming that reduction of the rate of transition to a post-hydrolytic stimulatory conformation would reduce K_{ATP} channel openings. To test this assumption, we analyzed the mechanism(s) by which ATPγS and AMP-PxP affect conformation switching. Substi-

tuted receptors with increased affinities for ATP were used to facilitate the analysis. Substitution of the SUR1 catalytic glutamate, Glu-1507, with glutamine, expected to drastically reduce enzymatic activity and thus conversion to ADP-bound intermediates, significantly increased the affinity for ATP, which enhanced, rather than impaired, conformational switching (Fig. 1).

The results show that ATPγS can efficiently switch the conformation of substituted SUR1, albeit the affinities for this analog are weaker than for ATP. The affinity of $SUR1_{E1507Q}$ for MgATPγS is ~30-fold weaker than for MgATP. Mg^{2+} is not required for switching, and thus reduced rates of hydrolysis are not a factor. The ATP γ-phosphate has multiple interactions with the NBDs, and thus the reduced affinities for ATPγS *versus* ATP imply that substitution of a sulfur atom for oxygen weakens one or more of these interactions. We suggest that the reduced stimulatory action of MgATPγS is a reflection of the reduced affinity of SUR1 for this analog rather than a slow rate of hydrolysis.

The interactions with AMP-PNP and AMP-PCP are more complex. Several studies showed that these nonhydrolyzable analogs alone fail to stimulate K_{ATP} channels, will inhibit ATP stimulated channels, and fail to support the action of channel agonists (23–30). The usual interpretation has been that these nonhydrolyzable analogs bind to SUR1 and prevent transition to ADP-bound stimulatory states. We thought initially that like ATPγS, AMP-PNP and AMP-PCP would bind to the SUR1 NBDs, support dimerization, and thus support conformational switching. However, an early study showed that AMP-PNP alone did not affect GBC binding, but could partially rescue or reverse ATP-induced switching (58). Extending these observations showed that MgAMP-PNP alone, at concentrations far in excess of the IC_{50} for MgATP, does not support conformational change, but will reverse ATP-induced switching. These results are consistent with a structural study of an asymmetric bacterial ABC protein, TM287-TM288 from *T. maritima*, which shows that one molecule of AMP-PNP binds to the noncanonical NBD, where it impairs subsequent NBD dimerization and thus switching to outward-facing conformations (36) and with data on cystic fibrosis transmembrane conductance regulator showing preferential binding at NBD1 (48, 49). An eight-state model (Fig. 4*C*) was used to make a semiquantitative estimate of the affinity of AMP-PNP for $SUR1_{E1507Q}$. Based on the structure of TM287-TM288 with a single AMP-PNP bound to the noncanonical NBD, the eight-state model assumes binding only at NBD1 at concentrations below 10 mM. Equilibrium conditions are assumed to hold for $SUR1_{E1507Q}$. A dissociation constant (K_A) ~1.2 μM for MgAMP-PNP binding to NBD1 was obtained.

The analysis of switching in $SUR1_{E1507Q}$ provides insight into factors affecting ATP binding. Mg^{2+} significantly increases the apparent affinity of SUR1 for nucleotides (see Ref. 31) (compare Fig. 1*A* with Fig. 1*B*), consistent with Mg^{2+} interacting with Glu-1507 and the γ-phosphate directly or via a bridging water molecule as observed in other ABC proteins (35, 62). To quantify the effect of Mg^{2+} on ATP binding in the absence of enzymatic activity, a four-state equilibrium model was used to compare the affinities of $SUR1_{E1507Q}$ for MgATP *versus* ATP^{4-}. The estimated dissociation constants (K_T) are 1 *versus* 94 μM, ± Mg^{2+}, respectively, *i.e.* Mg^{2+} increases the affinity ~100-fold, adding ~2.8 kcal/mol of binding energy.

A second observation is worth noting. The allosteric constant, β, in the four-state model is significantly greater for $SUR1_{E1507Q}$ than WT or any of the other mutant receptors. Typical values range from ~7 to 15, but the value for $SUR1_{E1507Q}$ is ~40 with or without Mg^{2+} present. The product, βK_G, reflects the affinity of the fully ATP-liganded receptor for GBC. Previous estimates for the affinities for GBC of WT, $SUR1_{Q1178R}$, and $SUR1_{R1182Q}$ in the ATP-bound outward-facing state showed that they were 10–12 times weaker than for the inward-facing conformation, *i.e.* ~10 nM *versus* 1 nM for the apo-receptors (31). Thus the affinity of ATP-bound $SUR1_{E1507Q}$ is ~25 nM (40 × 0.63 nM), reflected in the lower plateau values at saturating concentrations of ATP. The structural difference(s) responsible for this change are not clear, but we speculate that the $SUR1_{E1507Q}$ NBD dimer may be more compact, allowing a greater "twist" of the transmembrane helical domains, TMD1 and TMD2, that determine the GBC-binding pocket.

The E1507Q substitution has not been identified with disease to date, but its high affinity for ATP predicts that it would produce hyperactive channels. $SUR1_{E1507Q}$ has a somewhat reduced affinity for MgADP *versus* WT, but a more precise estimate is difficult because its affinity for ATP is high and it is hard to suppress the endogenous adenylate kinase in our membrane preparations. The results are consistent with electrophysiologic data on the E1507D substitution that, when assembled with Kir6.2, produces hyperactive K_{ATP} channels that are less sensitive to stimulation by MgADP (52).

In summary, the present results demonstrate the need to reinterpret early results that suggested that ATP analogs modulate K_{ATP} channel activity by affecting ATP hydrolysis. The present data suggest that ATPγS is less effective than ATP because SUR1 binds it less tightly, whereas AMP-PNP and AMP-PCP interact with asymmetric SUR1 via selective binding to NBD1 that prevents NBD dimerization and thus conformational switching.

REFERENCES

1. Aguilar-Bryan, L., and Bryan, J. (1999) Molecular biology of adenosine triphosphate-sensitive potassium channels. *Endocr. Rev.* **20,** 101–135
2. Pratt, E. B., and Shyng, S. L. (2011) ATP activates ATP-sensitive potassium channels composed of mutant sulfonylurea receptor 1 and Kir6.2 with diminished PIP_2 sensitivity. *Channels (Austin)* **5,** 314–319
3. Pratt, E. B., Tewson, P., Bruederle, C. E., Skach, W. R., and Shyng, S. L. (2011) N-terminal transmembrane domain of SUR1 controls gating of Kir6.2 by modulating channel sensitivity to PIP_2. *J. Gen. Physiol.* **137,** 299–314
4. Shyng, S. L., Barbieri, A., Gumusboga, A., Cukras, C., Pike, L., Davis, J. N., Stahl, P. D., and Nichols, C. G. (2000) Modulation of nucleotide sensitivity of ATP-sensitive potassium channels by phosphatidylinositol-4-phosphate 5-kinase. *Proc. Natl. Acad. Sci. U.S.A.* **97,** 937–941
5. Shyng, S. L., and Nichols, C. G. (1998) Membrane phospholipid control of nucleotide sensitivity of K_{ATP} channels. *Science* **282,** 1138–1141
6. Baukrowitz, T., and Fakler, B. (2000) K_{ATP} channels gated by intracellular nucleotides and phospholipids. *Eur. J. Biochem.* **267,** 5842–5848
7. Baukrowitz, T., Schulte, U., Oliver, D., Herlitze, S., Krauter, T., Tucker, S. J., Ruppersberg, J. P., and Fakler, B. (1998) PIP_2 and PIP as determinants for ATP inhibition of K_{ATP} channels. *Science* **282,** 1141–1144

8. Enkvetchakul, D., Loussouarn, G., Makhina, E., Shyng, S. L., and Nichols, C. G. (2000) The kinetic and physical basis of K_{ATP} channel gating: toward a unified molecular understanding. *Biophys. J.* **78,** 2334–2348
9. Fan, Z., and Makielski, J. C. (1999) Phosphoinositides decrease ATP sensitivity of the cardiac ATP-sensitive K^+ channel. A molecular probe for the mechanism of ATP-sensitive inhibition. *J. Gen. Physiol.* **114,** 251–269
10. Bränström, R., Corkey, B. E., Berggren, P. O., and Larsson, O. (1997) Evidence for a unique long chain acyl-CoA ester binding site on the ATP-regulated potassium channel in mouse pancreatic beta cells. *J. Biol. Chem.* **272,** 17390–17394
11. Bränström, R., Leibiger, I. B., Leibiger, B., Corkey, B. E., Berggren, P. O., and Larsson, O. (1998) Long chain coenzyme A esters activate the pore-forming subunit (Kir6. 2) of the ATP-regulated potassium channel. *J. Biol. Chem.* **273,** 31395–31400
12. Gribble, F. M., Proks, P., Corkey, B. E., and Ashcroft, F. M. (1998) Mechanism of cloned ATP-sensitive potassium channel activation by oleoyl-CoA. *J. Biol. Chem.* **273,** 26383–26387
13. Bränström, R., Aspinwall, C. A., Välimäki, S., Ostensson, C. G., Tibell, A., Eckhard, M., Brandhorst, H., Corkey, B. E., Berggren, P. O., and Larsson, O. (2004) Long-chain CoA esters activate human pancreatic beta-cell K_{ATP} channels: potential role in Type 2 diabetes. *Diabetologia* **47,** 277–283
14. Schulze, D., Rapedius, M., Krauter, T., and Baukrowitz, T. (2003) Long-chain acyl-CoA esters and phosphatidylinositol phosphates modulate ATP inhibition of KATP channels by the same mechanism. *J. Physiol.* **552,** 357–367
15. Riedel, M. J., Boora, P., Steckley, D., de Vries, G., and Light, P. E. (2003) Kir6.2 polymorphisms sensitize beta-cell ATP-sensitive potassium channels to activation by acyl CoAs: a possible cellular mechanism for increased susceptibility to type 2 diabetes? *Diabetes* **52,** 2630–2635
16. Best, L., Jarman, E., and Brown, P. D. (2011) A dual action of saturated fatty acids on electrical activity in rat pancreatic beta-cells. Role of volume-regulated anion channel and K_{ATP} channel currents. *J. Physiol.* **589,** 1307–1316
17. de Wet, H., Mikhailov, M. V., Fotinou, C., Dreger, M., Craig, T. J., Vénien-Bryan, C., and Ashcroft, F. M. (2007) Studies of the ATPase activity of the ABC protein SUR1. *FEBS J.* **274,** 3532–3544
18. Mikhailov, M. V., Campbell, J. D., de Wet, H., Shimomura, K., Zadek, B., Collins, R. F., Sansom, M. S., Ford, R. C., and Ashcroft, F. M. (2005) 3-D structural and functional characterization of the purified K_{ATP} channel complex Kir6.2-SUR1. *EMBO J.* **24,** 4166–4175
19. Zingman, L. V., Alekseev, A. E., Bienengraeber, M., Hodgson, D., Karger, A. B., Dzeja, P. P., and Terzic, A. (2001) Signaling in channel/enzyme multimers: ATPase transitions in SUR module gate ATP-sensitive K^+ conductance. *Neuron* **31,** 233–245
20. Aittoniemi, J., Fotinou, C., Craig, T. J., de Wet, H., Proks, P., and Ashcroft, F. M. (2009) Review. SUR1: a unique ATP-binding cassette protein that functions as an ion channel regulator. *Philos. Trans. R Soc. Lond. B Biol. Sci.* **364,** 257–267
21. Alekseev, A. E., Hodgson, D. M., Karger, A. B., Park, S., Zingman, L. V., and Terzic, A. (2005) ATP-sensitive K^+ channel channel/enzyme multimer: metabolic gating in the heart. *J. Mol. Cell. Cardiol.* **38,** 895–905
22. Matsuo, M., Kimura, Y., and Ueda, K. (2005) K_{ATP} channel interaction with adenine nucleotides. *J. Mol. Cell. Cardiol.* **38,** 907–916
23. Findlay, I. (1987) ATP-sensitive K^+ channels in rat ventricular myocytes are blocked and inactivated by internal divalent cations. *Pflugers Arch.* **410,** 313–320
24. Findlay, I. (1988) Effects of ADP upon the ATP-sensitive K^+ channel in rat ventricular myocytes. *J. Membr. Biol.* **101,** 83–92
25. Dunne, M. J. (1989) Protein phosphorylation is required for diazoxide to open ATP-sensitive potassium channels in insulin (RINm5F) secreting cells. *FEBS Lett.* **250,** 262–266
26. Dunne, M. J., Aspinall, R. J., and Petersen, O. H. (1990) The effects of cromakalim on ATP-sensitive potassium channels in insulin-secreting cells. *Br. J. Pharmacol.* **99,** 169–175
27. Ashcroft, F. M., and Kakei, M. (1989) ATP-sensitive K^+ channels in rat pancreatic beta-cells: modulation by ATP and Mg^{2+} ions. *J. Physiol.* **416,** 349–367
28. Takano, M., Qin, D. Y., and Noma, A. (1990) ATP-dependent decay and recovery of K^+ channels in guinea pig cardiac myocytes. *Am. J. Physiol.* **258,** H45–50
29. Treherne, J. M., and Ashford, M. L. (1992) Extracellular cations modulate the ATP sensitivity of ATP-K^+ channels in rat ventromedial hypothalamic neurons. *Proc. Biol. Sci.* **247,** 121–124
30. Schwanstecher, M., Sieverding, C., Dörschner, H., Gross, I., Aguilar-Bryan, L., Schwanstecher, C., and Bryan, J. (1998) Potassium channel openers require ATP to bind to and act through sulfonylurea receptors. *EMBO J.* **17,** 5529–5535
31. Ortiz, D., Voyvodic, P., Gossack, L., Quast, U., and Bryan, J. (2012) Two Neonatal diabetes mutations on transmembrane helix 15 of SUR1 increase affinity for ATP and ADP at nucleotide binding domain 2. *J. Biol. Chem.* **287,** 17985–17995
32. Higgins, C. F., and Linton, K. J. (2004) The ATP switch model for ABC transporters. *Nat. Struct. Mol. Biol.* **11,** 918–926
33. Rees, D. C., Johnson, E., and Lewinson, O. (2009) ABC transporters: the power to change. *Nat. Rev. Mol. Cell. Biol.* **10,** 218–227
34. Dawson, R. J., and Locher, K. P. (2007) Structure of the multidrug ABC transporter Sav1866 from Staphylococcus aureus in complex with AMP-PNP. *FEBS Lett.* **581,** 935–938
35. Oldham, M. L., and Chen, J. (2011) Snapshots of the maltose transporter during ATP hydrolysis. *Proc. Natl. Acad. Sci. U.S.A.* **108,** 15152–15156
36. Hohl, M., Briand, C., Grütter, M. G., and Seeger, M. A. (2012) Crystal structure of a heterodimeric ABC transporter in its inward-facing conformation. *Nat. Struct. Mol. Biol.* **19,** 395–402
37. Lubelski, J., van Merkerk, R., Konings, W. N., and Driessen, A. J. (2006) Nucleotide-binding sites of the heterodimeric LmrCD ABC-multidrug transporter of *Lactococcus lactis* are asymmetric. *Biochemistry* **45,** 648–656
38. Procko, E., Ferrin-O'Connell, I., Ng, S. L., and Gaudet, R. (2006) Distinct structural and functional properties of the ATPase sites in an asymmetric ABC transporter. *Mol. Cell.* **24,** 51–62
39. Qin, L., Zheng, J., Grant, C. E., Jia, Z., Cole, S. P., and Deeley, R. G. (2008) Residues responsible for the asymmetric function of the nucleotide binding domains of multidrug resistance protein 1. *Biochemistry* **47,** 13952–13965
40. Procko, E., O'Mara, M. L., Bennett, W. F., Tieleman, D. P., and Gaudet, R. (2009) The mechanism of ABC transporters: general lessons from structural and functional studies of an antigenic peptide transporter. *FASEB J.* **23,** 1287–1302
41. Christesen, H. B. T., Sjöblad, S., Brusgaard, K., Papadopoulou, D., and Jacobsen, B. B. (2005) Permanent neonatal diabetes in a child with an ABCC8 gene mutation. *Hormone Res.* **64,** Suppl. 1, 135
42. Babenko, A. P. (2008) A novel ABCC8 (SUR1)-dependent mechanism of metabolism-excitation uncoupling. *J. Biol. Chem.* **283,** 8778–8782
43. Tombline, G., Bartholomew, L. A., Tyndall, G. A., Gimi, K., Urbatsch, I. L., and Senior, A. E. (2004) Properties of P-glycoprotein with mutations in the "catalytic carboxylate" glutamate residues. *J. Biol. Chem.* **279,** 46518–46526
44. Orelle, C., Dalmas, O., Gros, P., Di Pietro, A., and Jault, J. M. (2003) The conserved glutamate residue adjacent to the Walker-B motif is the catalytic base for ATP hydrolysis in the ATP-binding cassette transporter BmrA. *J. Biol. Chem.* **278,** 47002–47008
45. Oldham, M. L., Khare, D., Quiocho, F. A., Davidson, A. L., and Chen, J. (2007) Crystal structure of a catalytic intermediate of the maltose transporter. *Nature* **450,** 515–521
46. Smith, P. C., Karpowich, N., Millen, L., Moody, J. E., Rosen, J., Thomas, P. J., and Hunt, J. F. (2002) ATP binding to the motor domain from an ABC transporter drives formation of a nucleotide sandwich dimer. *Mol. Cell* **10,** 139–149
47. Moody, J. E., Millen, L., Binns, D., Hunt, J. F., and Thomas, P. J. (2002) Cooperative, ATP-dependent association of the nucleotide binding cassettes during the catalytic cycle of ATP-binding cassette transporters. *J. Biol. Chem.* **277,** 21111–21114
48. Aleksandrov, L., Aleksandrov, A. A., Chang, X. B., and Riordan, J. R. (2002) The first nucleotide binding domain of cystic fibrosis transmembrane conductance regulator is a site of stable nucleotide interaction, whereas

the second is a site of rapid turnover. *J. Biol. Chem.* **277,** 15419–15425
49. Aleksandrov, L., Mengos, A., Chang, X., Aleksandrov, A., and Riordan, J. R. (2001) Differential interactions of nucleotides at the two nucleotide binding domains of the cystic fibrosis transmembrane conductance regulator. *J. Biol. Chem.* **276,** 12918–12923
50. Löffler-Walz, C., and Quast, U. (1998) Binding of K_{ATP} channel modulators in rat cardiac membranes. *Br. J. Pharmacol.* **123,** 1395–1402
51. Wyman, J., and Gill, S.J.(1990) *Binding and Linkage: Functional Chemistry of Biological Macromolecules,* University Science Books, Mill Valley, CA
52. Männikkö, R., Flanagan, S. E., Sim, X., Segal, D., Hussain, K., Ellard, S., Hattersley, A. T., and Ashcroft, F. M. (2011) Mutations of the same conserved glutamate residue in NBD2 of the sulfonylurea receptor 1 subunit of the K_{ATP} channel can result in either hyperinsulinism or neonatal diabetes. *Diabetes* **60,** 1813–1822
53. Yount, R. G. (1975) ATP analogs. *Adv. Enzymol. Relat. Areas Mol. Biol.* **43,** 1–56
54. Hehl, S., and Neumcke, B. (1994) K_{ATP} channels of mouse skeletal muscle: mechanism of channel blockage by AMP-PNP. *Eur. Biophys. J.* **23,** 231–237
55. Lederer, W. J., and Nichols, C. G. (1989) Nucleotide modulation of the activity of rat heart ATP-sensitive K^+ channels in isolated membrane patches. *J. Physiol.* **419,** 193–211
56. Schwanstecher, C., Dickel, C., and Panten, U. (1994) Interaction of tolbutamide and cytosolic nucleotides in controlling the ATP-sensitive K^+ channel in mouse beta-cells. *Br. J. Pharmacol.* **111,** 302–310
57. Proks, P., de Wet, H., and Ashcroft, F. M. (2010) Activation of the K_{ATP} channel by Mg-nucleotide interaction with SUR1. *J. Gen. Physiol.* **136,** 389–405
58. Schwanstecher, M., Löser, S., Brandt, C., Scheffer, K., Rosenberger, F., and Panten, U. (1992) Adenine nucleotide-induced inhibition of binding of sulphonylureas to their receptor in pancreatic islets. *Br. J. Pharmacol.* **105,** 531–534
59. Matsuo, M., Kioka, N., Amachi, T., and Ueda, K. (1999) ATP binding properties of the nucleotide-binding folds of SUR1. *J. Biol. Chem.* **274,** 37479–37482
60. Ueda, K., Inagaki, N., and Seino, S. (1997) MgADP antagonism to Mg^{2+}-independent ATP binding of the sulfonylurea receptor SUR1. *J. Biol. Chem.* **272,** 22983–22986
61. Cheng, Y., and Prusoff, W. H. (1973) Relationship between the inhibition constant (K_1) and the concentration of inhibitor which causes 50 per cent inhibition (I_{50}) of an enzymatic reaction. *Biochem. Pharmacol.* **22,** 3099–3108
62. Hung, L. W., Wang, I. X., Nikaido, K., Liu, P. Q., Ames, G. F., and Kim, S. H. (1998) Crystal structure of the ATP-binding subunit of an ABC transporter. *Nature* **396,** 703–707